SUPPLEMENTARY MATERIALS

Abbreviations: AAN = ascending arousal network; ARAS = ascending reticular activating system; CEM/Pf = centromedian/parafascicular nucleus of the thalamus; CHN = central homeostatic network; CL = central lateral nucleus of the thalamus; CnF = cuneiform nucleus; CTT = central tegmental tract; dAAN = default ascending arousal network; DBB = diagonal band of Broca; DMN = default mode network; DR = dorsal raphe; DTT = dorsal tegmental tract; DTT_L = dorsal tegmental tract, lateral division; DTT_M = dorsal tegmental tract, medial division; DWI = diffusion-weighted imaging; EEG = electroencephalography; FA = fractional anisotropy; fMRI = functional magnetic resonance imaging; IC = inferior colliculus; LC = locus coeruleus; LDTg = laterodorsal tegmental nucleus; LFB = lateral forebrain bundle; LHA = lateral hypothalamic area; MFB = medial forebrain bundle; ML = medial lemniscus; MLF = medial longitudinal fasciculus; MnR = median raphe; MPFC = medial prefrontal cortex; MRI = magnetic resonance imaging; mRt = mesencephalic reticular formation; NBM = nucleus basalis of Meynert; PAG; periaqueductal grey; PBC = parabrachial complex; PBP = parabrachial pigmented nucleus of the ventral tegemental area; PComm = posterior commissure; PIF = parainterfascicular nucleus; PMC = postero-medial complex (i.e. posterior cingulate and precuneus); PN = paranigral nucleus of ventral tegmental area; PnO = pontine reticular nucleus = oral part (pontis oralis); PTg = pedunculotegmental nucleus; PV = paraventricular nucleus of the thalamus; Ret = reticular nucleus of the thalamus; RIs = retroisthmic nucleus; RLi = rostral linear nucleus; RMg = raphe magnus; SC = superior colliculus; SCP = superior cerebellar peduncle; SI = substantia innominata; SN = substantia nigra; TM = tuberomammillary nucleus; VLPO = ventrolateral pre-optic area; VTA = ventral tegmental area; VTAR = ventral tegmental area, rostral part; VTT = ventral tegmental tract; VTT_C = ventral tegmental tract, caudal division; VTT_R = ventral tegmental tract, rostral division.

SUPPLEMENTARY METHODS

A representative animal electrophysiological study of arousal

In 1982, Steriade and colleagues tested the hypothesis generated by Moruzzi and Magoun in 1949 that the brainstem reticular formation drives tonic activation of thalamocortical circuits, and therefore cortical EEG desynchronization, by increasing firing rates during wakefulness versus slow-wave sleep (*35*). Rather than using electrical stimulation or lesion-based techniques, Steriade and colleagues recorded extracellularly the spontaneous firing of mRt neurons while seven cats were awake, sleeping, or transitioning between these states, as determined by cortical EEG patterns. MRt neuron firing rates were significantly higher during wakefulness than sleep. This finding was most prominent in mRt neurons projecting rostrally versus caudally (i.e., to the paramedian pons). Moreover, the increase in firing rate corresponded to EEG and behavioral evidence of wakefulness and was tonic in nature, suggesting a direct link between mRt activity, activation of the cortical EEG, and behavioral evidence of wakefulness. These results suggest that the mRt plays an important role in sustaining wakefulness as part of the dAAN.

Overview of neuroanatomic localization of candidate dAAN nodes

To facilitate reproduction of our methods, we describe the neuroanatomic boundaries of the candidate brainstem dAAN nodes in **Tables S1-S5**. In addition, we detail our approach to defining the neuroanatomic borders of each nucleus. We use the Paxinos atlas as our primary reference (*48*), but we also consider differences between the Paxinos atlas and the Olszewski and Baxter brainstem atlas (*50*), another canonical brainstem atlas of human neuronanatomy. Where applicable, we explain our rationale for mediating discrepancies in anatomic borders and/or nomenclature between these atlases, as well as between these atlases and other neuroanatomic

studies. Finally, we explain for each brainstem dAAN node how the nomenclature and borders proposed here differ from those that our laboratory has used previously (*9, 54, 99, 109, 151*), including in our prior analyses of Specimen 1 (*9, 99*). At the completion of this process, we updated the Harvard Ascending Arousal Network Atlas and now release version 2.0 of the atlas (doi:10.5061/dryad.zw3r228d2; download link: https://datadryad.org/stash/share/aJ713eXY12ND56bzOBejVG2jmOFCD2CKxdSJsYWEHkw).

Neuroanatomic localization of midbrain dAAN nodes

Mesencephalic Reticular Formation (mRt):

The mRt is a region of the midbrain tegmentum that has been described using multiple names and as containing multiple subnuclei by different neuroanatomists. In Olszewski and Baxter's atlas, the most caudal aspect of the midbrain tegmentum, at the level of the isthmus, contains the cuneiform nucleus (CNF). The remainder of the caudal midbrain tegmentum, at the level of the decussation of the SCP, contains the mesencephalic reticular formation (MRF) and the mesencephalic reticular formation, ventral part (MRFv). Olszewski's MRF nucleus continues rostrally and traverses the entire rostro-caudal extent of the midbrain, up to the mesencephalic-diencephalic junction. The MRFv's rostral border ends at the mid-level of the red nuclei. In the rostral midbrain, at the level of the red nuclei, a small intracuneiform nucleus (ICUN) is shown within the MRF.

In Paxinos' atlas, the most caudal aspect of the midbrain tegmentum, at the level of the isthmus, similarly contains CnF. However, another subnucleus named the isthmic reticular formation (isRt) is located in this region dorsal to the pedunculotegmental nucleus (PTg) and ventral to the CnF. In Paxinos' atlas, the remainder of the caudal midbrain tegmentum, at the

level of the decussation of the SCP, contains the CnF and isRt. At the transition from the decussation of the SCP to the red nuclei, the CnF and isRt nomenclature changes to the precuneiform area (PrCnF) and mesencephalic reticular formation (mRt), respectively. In the rostral midbrain, at the level of the red nuclei, the entire tegmentum is comprised of the mRt, which extends from the PAG on its dorso-medial border to the medial lemniscus on its ventro-lateral border. Within the rostral portion of the mRt, Paxinos defines a small subnucleus called the central mesencephalic nucleus (CeMe) in the same region that Olszewski defines the ICUN. Finally, at the mesencephalic-diencephalic junction, Paxinos' mRt becomes the p1 reticular formation (p1Rt) (plates 8.62 to 8.64).

In summary, Olszewski and Paxinos describe a similar region of the midbrain tegmentum as containing a cluster of arousal nuclei, albeit with different nomenclature and different subnuclei. The region of the midbrain tegmentum that is described by Olszewski as containing CNF, MRF, MRFv, and ICUN is described by Paxinos as containing CnF, isRt, PrCnF, mRt, CeMe, and p1Rt. In our prior work (*9*), we used the term cuneiform/subcuneiform nucleus (CSC) to describe this region. We traced it in the rostral midbrain, in deference to Moruzzi and Magoun's seminal study in which stimulation of the rostral midbrain tegmentum led to arousal and cortical activation in lightly anesthetized cats (*13*). We now update our nomenclature from CSC to mRt to ensure consistency with the Paxinos atlas' nomenclature. Furthermore, we have extended our mRt region of interest (ROI) to include all of the aforementioned subnuclei described by Olszewski and Paxinos, such that our mRt ROI now extends throughout the entire rostro-caudal axis of the midbrain tegmentum. Specifically, our mRt ROI contains all of the following subnuclei described by Paxinos: CnF, isRt, PrCnF, mRt, CeMe, and p1Rt.

Periaqueductal Grey (PAG):

The anatomic borders and contours of our PAG ROI are consistent with those of the PAG described in Paxinos. We trace the PAG as a single ROI, which encompasses multiple subnuclei described in Paxinos. Specifically, our PAG ROI includes the following subnuclei described by Paxinos: lateral PAG (LPAG); dorsolateral PAG (DLPAG); dorsomedial PAG (DMPAG); pleioglia PAG (PlGl); and p1 PAG (p1PAG).

Pedunculotegmental Nucleus (PTg):

The PTg ROI contains both the pars compactus (called PTg by Paxinos) and the pars dissipatus (called the retroisthmic nucleus [RIs] by Paxinos). The pars dissipatus is called nucleus tegmenti pedunculopontinus, subnucleus dissipatus by Olszewski and the diffuse medial component of Ch5 by Mesulam (*196*). We have not changed our operational definition of neuroanatomic localization of the PTg, but we have updated our nomenclature from pedunculopontine nucleus (PPN) to PTg to ensure consistency with nomenclature of the Paxinos atlas. Our PTg ROI thus contains the PTg and RIs, as described by Paxinos. In addition, we made one edit to the boundaries of PTg in the Harvard AAN Atlas version 2.0, as compared to version 1.0: in version 2.0, we deleted one voxel in the PTg at MNI axial level z53 and reassigned this voxel to the VTA, based on tyrosine hydroxylase staining data and based on the anatomic boundaries in the Paxinos atlas.

Dorsal Raphe (DR):

The DR nucleus extends from the rostral pons to the caudal midbrain. We classify DR as a midbrain nucleus, because that is where most DR neurons are located. Paxinos shows DR

continuing rostrally past the caudal border of the red nuclei. However, in our experience studying human brainstem specimens, serotonergic DR neurons do not extend past the rostral border of the trochlear nucleus, which is at the caudal border of the red nucleus. Our DR ROI includes the following subnuclei described by Paxinos: DR, caudal part (DRC); DR, dorsal part (DRD); DR, interfascicular part (DRI); DR, lateral part (DRL); DR, ventral part (DRV); posterodorsal raphe nucleus (PDR).

Ventral Tegmental Area (VTA):

The VTA ROI used in this study has two major differences compared to the prior VTA ROI used by our group and with version 1.0 of the Harvard Ascending Arousal Network Atlas: 1) its lateral extent and 2) its rostral extent. In our prior work, we did not include the lateral wing-like extensions of the PBP, as shown in Paxinos and in Pearson (*197*), because this subregion is difficult to differentiate from the nearby substantia nigra. However, with our new tyrosine hydroxylase immunostaining (Figure 1) and with reference to the Paxinos atlas, we were able to make this distinction between PBP and SN for the present studies.

The VTA node proposed here also has a more rostral extent than the VTA ROI that we used in prior studies (*9, 99*). Previously, we based the neuroanatomic borders of the VTA on hematoxylin-and-eosin-stained sections from human brainstem specimens, which revealed the highest density of catecholamine neurons, as demonstrated by the presence of neuromelanin, in the caudal midbrain. However, we recognize that VTA neurons have been identified in the rostral mesencephalon by other laboratories using a variety of staining techniques, such as tyrosine hydroxylase (*86, 198*). Thus, we performed new tyrosine hydroxylase stains on four midbrain sections from Specimen 1 (https://histopath.nmr.mgh.harvard.edu). These stains

revealed a distribution of VTA neurons that was consistent with that described in the studies by Oades, Halliday, Pearson, and colleagues (**Figure 2**). Therefore, we use a VTA ROI in the present work that extends throughout the entire rostro-caudal axis of the midbrain. Finally, we do not include the rostral linear nucleus as part of the VTA, although some dopaminergic cells may reside in this region (*86*), because this nucleus is primarily serotonergic.

Finally, we edited the midline portion of the VTA node, based on the observation that VTA neurons in the midline of the midbrain were only seen at the level of the red nucleus, not at the level of the superior cerebellar peduncle. This immunostaining observation is consistent with the VTA anatomic borders in the Paxinos atlas along the rostro-caudal axis of the midbrain. Thus, we removed the midline VTA voxels at the level of the superior cerebellar peduncle in version 2.0 of the Harvard AAN atlas.

In summary, the VTA ROI used in this study contains the following nuclear subregions described by Paxinos: parainterfascicular nucleus (PIF); paranigral nucleus of ventral tegmental area (PN); ventral tegmental area (VTA); ventral tegmental area, rostral part (VTAR); and parabrachial pigmented nucleus of the VTA (PBP). This VTA ROI contains the A10 nuclei, as described by Oades and Halliday (*86*). The neuroanatomic borders of the VTA ROI contain the following subregions described by Olszewski: the paranigral nucleus (PNg), interfascicular nucleus (INF), parabrachial pigmented nucleus (PBP), and ventral tegmental area of Tsai (VTA).

Neuroanatomic localization of pontine dAAN nodes

Pontine Reticular Nucleus, Oral Part (i.e., Pontis Oralis; PnO):

We have not changed the neuroanatomic localization of this nucleus since our prior studies (*9*), but we have updated our nomenclature from PO to PnO to reflect the Paxinos atlas's

nomenclature. Our PnO nucleus includes the following subnuclei described by Olszewski: nucleus reticularis pontis oralis (NRPO) and nucleus reticularis tegmenti pontis (NRTP). Paxinos does not subdivide PnO into these two subnuclei.

Parabrachial Complex (PBC):

The PBC is divided in the Paxinos atlas into medial and lateral components: medial parabrachial nucleus (MPB) and lateral parabrachial nucleus (LPB). MPB and LPB are further subdivided into subregions: MPB, external part (MPBE); LPB, central part (LPBC); LPB, dorsal part (LPBD); LPB, external part (LPBE); LPB, superior part (LPBS). Given the difficulty of delineating these subregions on MRI scans of the human brain, even at the ultra-high spatial resolution (~600 μm) at which Specimen 1 was imaged, we grouped all of these medial and lateral subregions into a single PBC node. This is the same approach that we used to delineate the PBC in our previous analyses of Specimen 1.

Of note, the caudal boundary of PBC in Paxinos (MPB) is located at plate 8.35, but we operationally define the caudal boundary to be located at the level of plate 8.37, which is the caudal border of the pontine arousal nuclei. Similarly, the rostral boundary of PBC in Paxinos' atlas is located at plate 8.49 but we operationally define the PBC as extending to plate 8.50, which is the transition point between PBC and PTg at the ponto-mesencephalic junction.

Median Raphe Nucleus (MnR):

In accordance with the terminology used by Paxinos, we define the MnR as comprising both the MnR proper and the slightly more lateral subnucleus, the paramedian raphe nucleus (PMnR). The PMnR begins in the midpons on plate 8.38, ventral to the dorsal raphe and medial to the

nucleus pontis oralis. It is joined medially by the MnR on plate 8.44 and disappears prior to the isthmus, on plate 8.48. The MnR continues rostrally into the caudal midbrain, ending at the level of the decussation of the superior cerebellar peduncle. As with the PBC (above), we operationally define the caudal and rostral boundaries of our MnR ROI as plates 8.37 and 8.50, respectively, since these are the anatomic levels of the mid-pons and the ponto-mesencephalic junction. Our MnR ROI encompasses the MnR and paramedian raphe nucleus.

Locus Coeruleus (LC):

This small, tubular nucleus begins in the dorsolateral midpons, on Paxinos plate 8.37, lateral to the fourth ventricle and medial to the superior cerebellar peduncle. It extends rostrally to the isthmus on plate 8.49. As with PBC and MnR above, we operationally consider the LC as extending to 8.50, which is the ponto-mesencephalic junction. The neuroanatomic location, borders and nomenclature for LC are similar in the Olszewski and Paxinos atlases.

Laterodorsal Tegmental Nucleus (LDTg):

Using Paxinos' terminology, we do not include the ventral nucleus, which is labeled the laterodorsal tegmental nucleus, ventral part (LDTgV), as part of our annotation of the LDTg. The LDTg is immediately adjacent to the medial edge of the LC. It lies dorsal to the medial longitudinal fasiculus (mLF), while the LDTgV is the subarea ventral to the mLF. It begins several levels rostral to the mid-pons (plate 8.41) and terminates at the level of the trochlear nucleus (8.51). As with PBC, MnR, and LC above, we operationally consider the LDTg as extending to 8.50, which is the ponto-mesencephalic junction.

Neuroanatomic localization of thalamic dAAN nodes

Intralaminar Nuclei (ILN):

Using the terminology of the Ding Brain Atlas (*49*), this collection of thalamic subnuclei includes the central lateral (CL), central medial (CeM), paracentral (PC), central dorsal (CD), centromedian (CM), parafascicular (Pf), subparafasicular (SPf) and the fasiculosus (Fa) nuclei. These subnuclei form an arc with a ventro-posterior bulge and are bordered medially by the dorsomedial nucleus and laterally by ventral anterior nucleus, ventral posterior nucleus and pulvinar.

Reticular Nucleus (Ret):

The reticular thalamic nucleus includes the magnocellular (Rmc) and parvocellular (Rpc) divisions (*49*) and forms the anterior and lateral border of the thalamus. Posteriorly, at the level of the lateral geniculate nucleus, it is laterally separated from the pulvinar by a thin layer of white matter.

Paraventricular Thalamic Nucleus (PaV):

The paraventricular thalamic nucleus (PaV) lines the medial border of the thalamus. On its medial side is the third ventricle. On its lateral side are several different thalamic nuclei along its antero-posterior extent: anteriorly, the lateral border of PaV is formed by ILN and the anterior nuclear complex; posteriorly, the lateral border of PaV is formed by the mediodorsal nucleus of the thalamus. The superior border of PaV is formed by the stria medullaris of the thalamus, and the inferior border of PaV is formed by the midline nuclear complex.

Neuroanatomic localization of hypothalamic dAAN nodes

Lateral Hypothalamic Area (LHA):

This region is subdivided into anterior (LHAa), posterior (LHAp) and tuberal regions (LHAtub) and forms the lateral border of the hypothalamus with the substantia innominata of the basal forebrain (*49*). The anterior-most region is not depicted in the Allen atlas. The tuberal region begins posterior to the ventrolateral pre-optic area (VLPO) and is subdivided into a magnocellular nucleus (LHmc), accessory secretory cells (LHsc) and a pallidohypothalamic area (PalHy). The posterior region extends to the posterior border of the hypothalamus, dorsal to the mammillary bodies and includes the perifornical nucleus (PeF).

Tuberomammillary Nucleus (TM):

This nucleus has an anterior component within the LHAtub, just medial to the optic tract. Posteriorly, it sits laterally to the mammillary bodies and inferior to the LHAp.

Supramammillary Nucleus (SUM):

This nucleus is located superior to the mammillary body and mammillothalamic tract. It is bordered medially by the posterior hypothalamic nucleus and laterally by the LHA and the TMN.

Neuroanatomic localization of basal forebrain dAAN nodes

Basal Nucleus of Meynert/Substantia Innominata (BNM/SI):

The BNM and SI are identified as a single region in our studies, as they cannot be anatomically distinguished using MRI. They occupy the area lateral to the hypothalamus and ventral to the

pallidum, extending anteriorly to the level of the anterior commissure and posteriorly to the posterior boundary of the amygdala (*49*).

Nucleus of the Diagonal Band (NDB):

The NDB includes vertical and horizontal subdivisions. It exists in its vertical orientation anterior to the anterior commissure, in the midline, medial to the septal nucleus and nucleus accumbens. At the level of the anterior commissure, it condenses ventrally into its horizontal subdivision, forming the border between the hypothalamus and the SI (*49*).

Methodologic Considerations for Deterministic and Probabilistic Tractography

To ensure consistency across methods, we standardized the deterministic and probabilistic processing parameters wherever possible, as detailed in the main text.

Some processing parameters, however, were not standardized due to differences in the deterministic and probabilistic techniques. For example, in all deterministic experiments, fiber tracts were terminated when the angle between water diffusion vectors in adjacent voxels exceeded a threshold of 60˚. This angle threshold was previously identified by our group as providing a balance between tract sensitivity (i.e. identification of the brainstem's widely branching pathways) and tract specificity (i.e. reduction of false positive tracts) (*9, 54, 99*). In contrast, we and other groups typically use a more liberal angle threshold of 80˚ (curvature threshold = 0.2), for probabilistic experiments, consistent with the default setting in FSL's Diffusion Toolbox. Notably, a recent *ex vivo* probabilistic tractography study that compared the accuracy of fiber tract data in the macaque brain to "gold standard" tract-tracer data found that probabilistic tract accuracy was minimally affected when angle thresholds were in the range of

70-90˚ (*186*). Similarly, the accuracy of the probabilistic tractography data was not affected by varying the FA thresholds between 0.0-0.3.

We did not include a distance correction (e.g., the "-pd" function in FSL's probtrackx) in our *CP* calculations. Although the probability of a connection between two anatomic regions, as detected by tractography, may be associated with the distance between the regions (*199*), it is unknown whether this association is linear or exponential. Moreover, the type of distance correction that is appropriate for a given bundle of tracts likely depends upon multiple variables, including the number of voxels in the seed/target nodes, the number of other bundles that intersect the bundle of interest along its course, and the geometry of the bundle (e.g. its curvature and branching). From a statistical perspective, it is unclear if a single distance correction method can account for the effect of distance on connectivity measures for different bundles. Furthermore, empiric data from a recent *ex vivo* MRI study of the macaque brain, which tested linear and exponential distance correction methods, found that the accuracy of probabilistic tractography data against gold-standard tract-tracing data was not improved by either distance correction method (*186*). Thus, we did not correct for inter-nodal distance in our *CP* measurements.

Supplementary Videos

Video S1. The Harvard Ascending Arousal Network (AAN) Atlas – Version 2.0. AAN brainstem nodes are rendered in three dimensions and superimposed upon the MNI152 atlas in 1 mm isotropic space. For anatomic reference, the nodes are shown on an axial image at the level of the mid-pons, a sagittal image at the midline, and a coronal image at the splenium of the corpus callosum. Blue = locus coeruleus; yellow = parabrachial complex; green = median raphe; orange = laterodorsal tegmental nucleus; light blue = pontis oralis; turquoise = dorsal raphe; red = mesencephalic reticular formation; purple = pedunculotegmental nucleus; light purple = periaqueductal grey; pink = ventral tegmental area.

Video S2. Visualizing default ascending arousal network connectivity within the ventral tegmental area hub node. All candidate brainstem dAAN nodes and their tract end-points are shown from a dorsal perspective, as in Fig. 6, superimposed upon a coronal non-diffusion-weighted (*b=0*) image at the level of the mid-thalamus and an axial *b=0* image at the intercollicular level of the midbrain. Tract end-points appear as disks and represent the start-points and termination-points of each tract (i.e., there are two end-points per tract). All tract end-points are color-coded by the node from which they originate, and the nodes are rendered semi-transparent so that end-points can be seen within them.

As the video begins, tract end-points are seen within the semi-transparent brainstem candidate nodes: ventral tegmental area (VTA), periaqueductal grey (PAG), and mesencephalic reticular formation (mRt), pedunculotegmental nucleus (PTg), and parabrachial complex (PBC). As the video proceeds, the viewer's eye moves ventrally through the PAG. Once the viewer's eye emerges from the ventral surface of the PAG, the dorsomedial border of the VTA is seen, where tract end-points from multiple candidate brainstem dAAN nodes overlap within the VTA and along its dorsal border: pedunculotegmental, parabrachial complex, and dorsal raphe (PTg-PBC-DR); pontis oralis, DR, and PTg (PnO-DR-PTg); and PBC-mRt-PTg. Tract end-point overlap does not prove synaptic connectivity but indicates extensive connectivity via association pathways between ipsilateral and midline dAAN nodes with the VTA.

Supplementary Figures

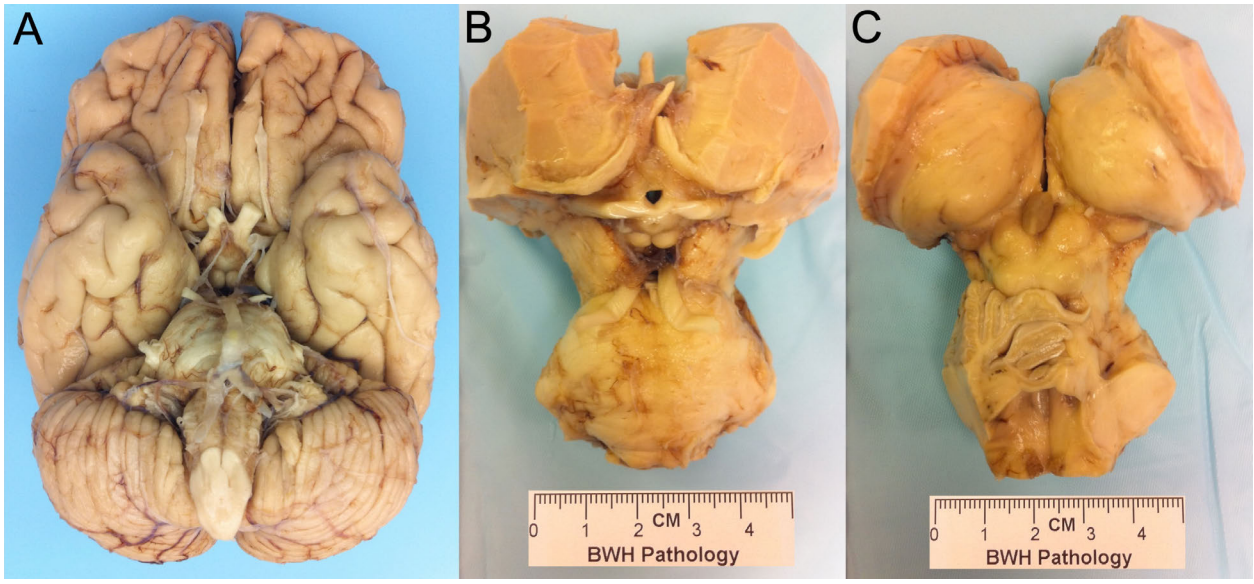

Fig. S1. Gross pathology photos of Specimen 1. (**A**) Inferior view of brain Specimen 1. The whole brain was dissected to a brainstem/diencephalon/forebrain specimen consisting of the pons, midbrain, hypothalamus, thalamus, basal forebrain, and portions of the basal ganglia, as shown from an (**B**) anterior and (**C**) posterior perspective. CM = centimeters. Figure adapted from Edlow et al. JNEN 2012 (*9*).

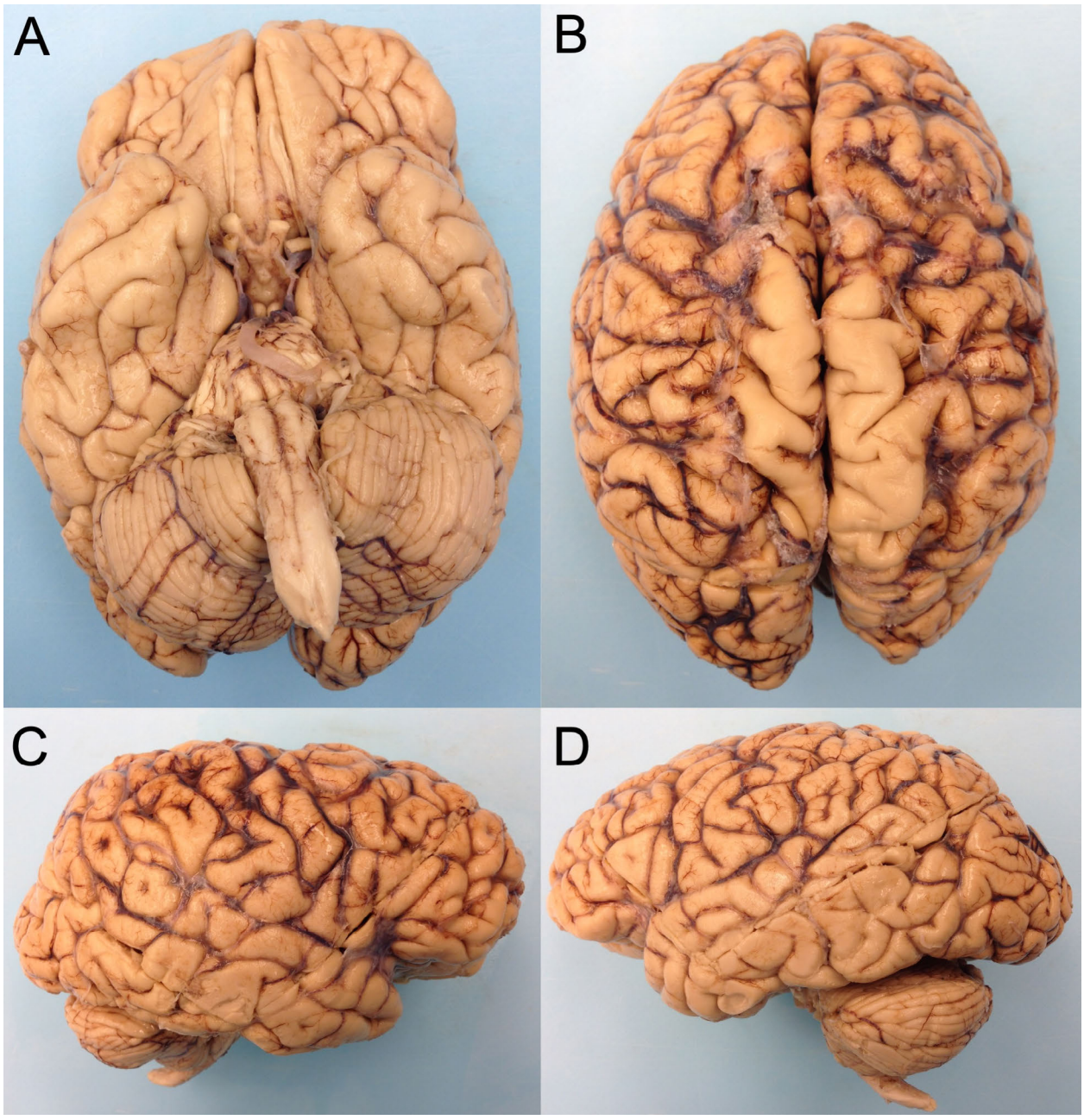

Fig. S2. Gross pathology photos of Specimen 2. Brain Specimen 2 is shown from an (**A**) inferior, (**B**) superior, (**C**) right lateral, and (**D**) left lateral perspective.

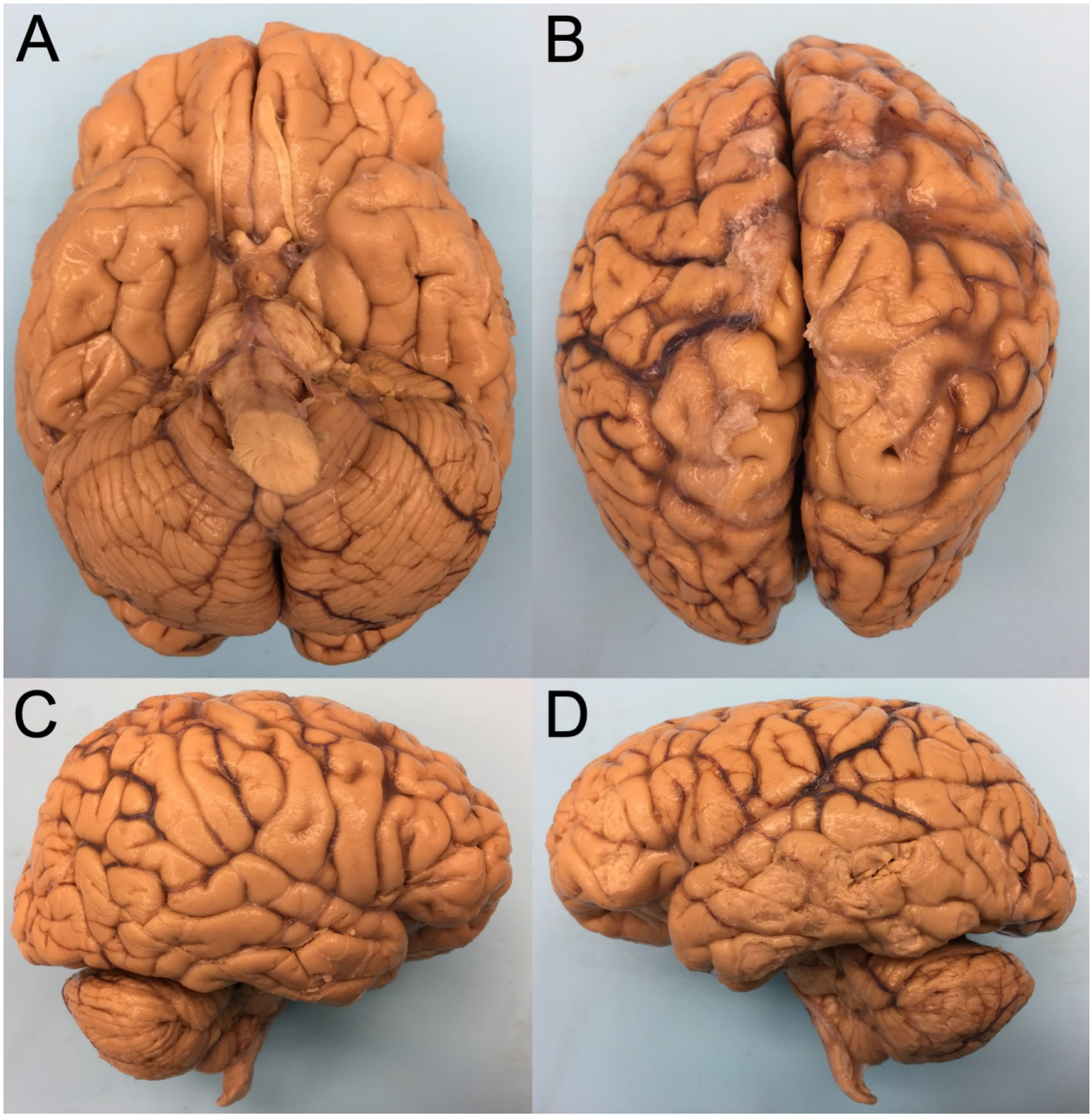

Fig. S3. Gross pathology photos of Specimen 3. Brain Specimen 3 is shown from an (**A**) inferior, (**B**) superior, (**C**) right lateral, and (**D**) left lateral perspective.

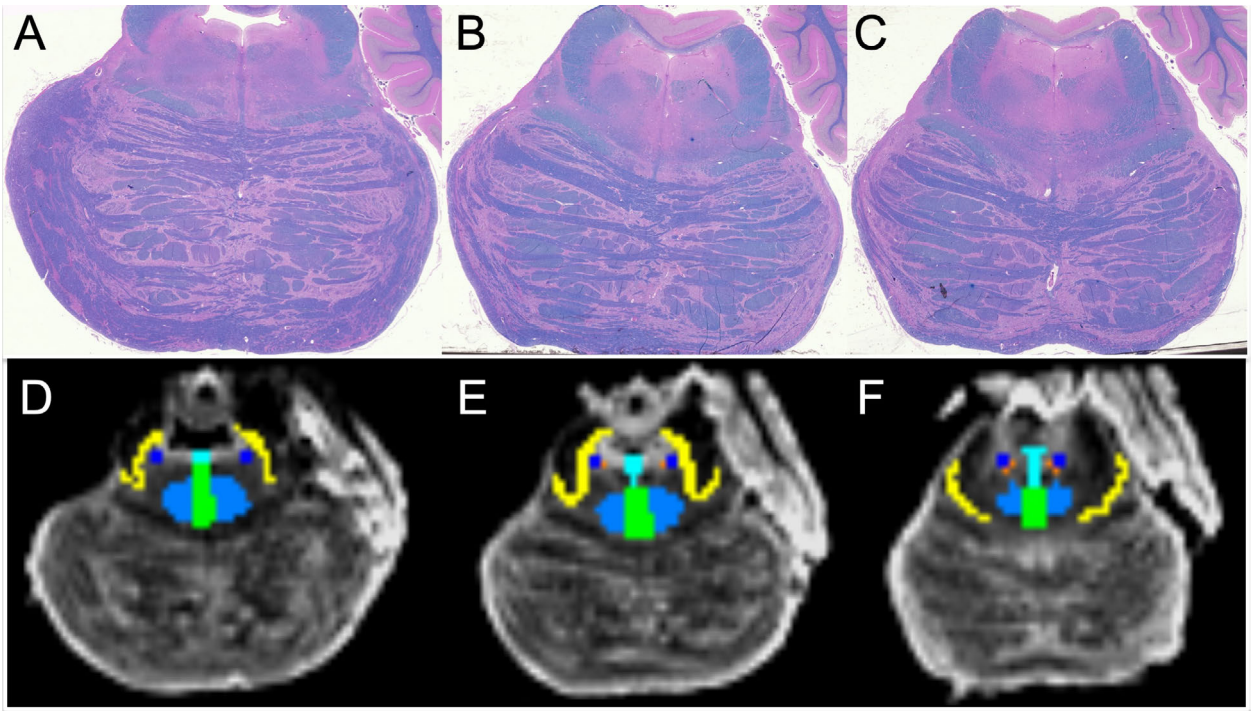

Fig S4. Neuroanatomic Localization of Pontine Arousal Nuclei. Axial histologic sections through the mid pons (**A**), upper pons (**B**) and rostral pons (**C**) for Specimen 1. Each section is stained with hematoxylin and eosin/Luxol fast blue. Corresponding axial non-diffusion-weighted (*b=0*) images (**D, E, F**). Regions of interest for tractography are traced on the *b=0* images with neuroanatomic borders determined by the histological stains: light blue = pontis oralis; turquoise = dorsal raphe; dark blue = locus coeruleus; yellow = parabrachial complex; green = median raphe; orange = laterodorsal tegmental nucleus. Figure adapted from Edlow et al. JNEN 2012 (*9*).

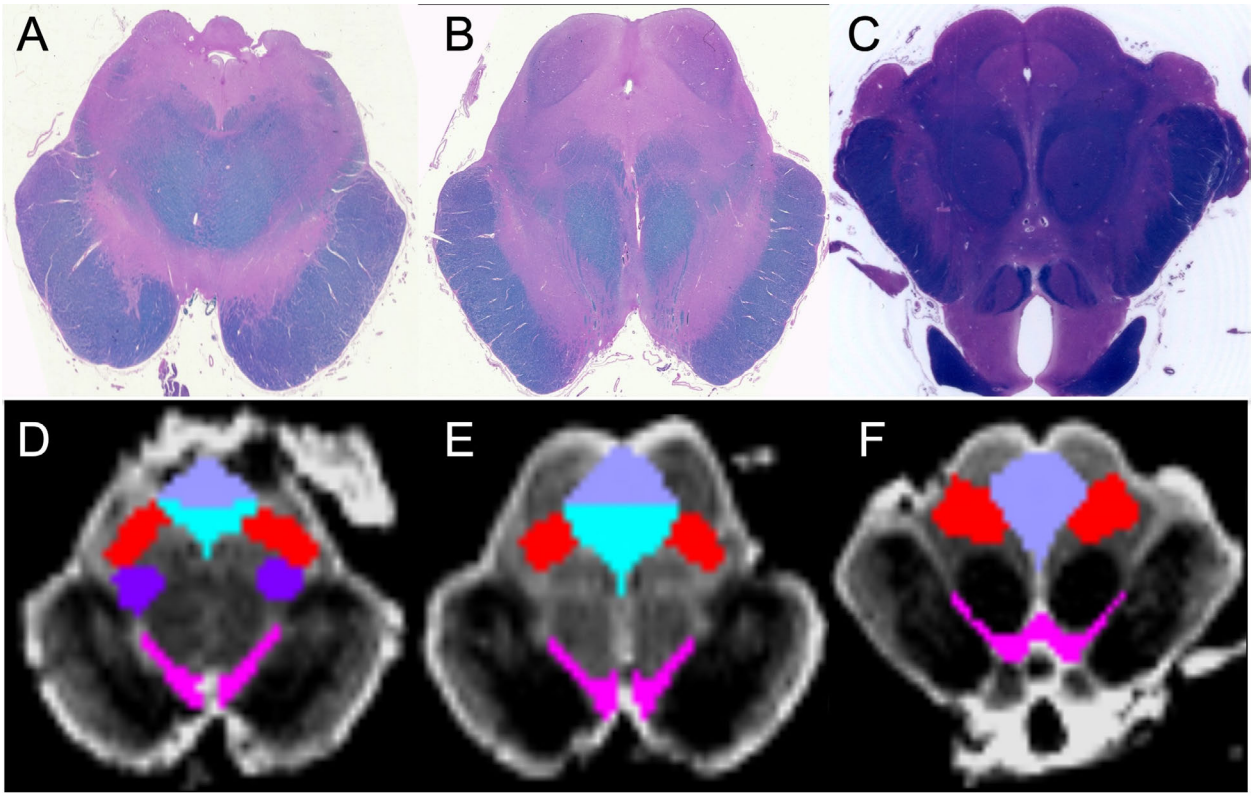

Fig. S5. Neuroanatomic Localization of Midbrain Arousal Nuclei. Axial histologic sections through the midbrain at the level of the decussation of the superior cerebellar peduncles (**A**), at the level of the inferior colliculi (**B**) and at the level of the superior colliculi and red nuclei (**C**) in Specimen 1. All sections are stained with hematoxylin and eosin/Luxol fast blue. Corresponding axial non-diffusion-weighted (*b=0*) images (**D, E, F**). Regions of interest for tractography are traced on the *b=0* images with neuroanatomic borders determined by the histological stains: red = mesencephalic reticular formation; pink = ventral tegmental area; dark purple = pedunculotegmental nucleus; turquoise = dorsal raphe; light purple = periaqueductal grey. Figure adapted from Edlow et al. JNEN 2012 (*9*).

Supplementary Tables

Table S1. Demographic and clinical characteristics for individuals who donated brain specimens

Specimen ID	Age	Sex	Medical History	Cause of Death	Fresh brain weight*	Post-mortem fixation interval	Post-mortem MRI interval	Type of MRI
Specimen 1	53	F	Pelvic sarcoma (high grade), breast carcinoma (stage 1), deep vein thrombosis, hypertension	Systemic complications of cancer	1250 grams	24 hours	103 days	4.7 Tesla Dissected Specimen
Specimen 2	60	F	Cecal adenocarcinoma (metastatic), deep vein thrombosis, depression	Septic shock	1440 grams	24 hours	719 days	3 Tesla Whole Brain Specimen
Specimen 3	61	F	Ovarian carcinoma (metastatic), hypertension	Septic shock	1305 grams	72 hours	609 days	

* Normal fresh brain weight = 1200-1500 grams.

Table S2. Neuroanatomic Localization of Midbrain Arousal Nuclei

Node	Component Nuclei	Atlas Plates	Rostral Boundary	Caudal Boundary	Ventral Boundary	Dorsal Boundary	Medial Boundary	Lateral Boundary
mRt	CnF, isRt, PrCnF, mRt, CeMe, and p1Rt	8.51 to 8.64	Mesencephalic-diencephalic junction	Ponto-mesencephalic junction	Caudal: CTg and PTg Rostral: CTg and ML	Caudal: IC Rostral: SC	Caudal: DR and PAG Rostral: PAG	Caudal: ML and IC Rostral: ML
VTA	PIF, PN, PBP, VTA, VTAR	8.51 to 8.64	Mesencephalic-diencephalic junction	Ponto-mesencephalic junction	Caudal: Interpeduncular nucleus Rostral: interpeduncular nucleus, fasciculus retroflexus, and interpeduncular fossa	Caudal: Decussation of the superior cerebellar peduncles Rostral: RLi (medially) and red nuclei (laterally)	Caudal: interpeduncular nucleus and caudal linear nucleus of the raphe Rostral: N/A	Caudal: trigeminothalamic tract, medial lemniscus and SN Rostral: SN
PAG	LPAG, DLPAG, DMPAG, PlGl, P1PAG	8.51 to 8.64	mesencephalic-diencephalic junction	Ponto-mesencephalic junction	Caudal: DR Rostral: Rli	Caudal: IC Rostral: SC and Pcomm	N/A	mRt
PTg	PTg, RIs	8.48 to 8.53	mRt (isRt)	PBC (LPBC)	Trigeminothalamic tract and retrorubral field	mRt and spinothalamic tract	Caudal: Decusation of superior cerebellar peduncles Rostral: CTg	Ventral: Trigeminothalamic tract and ML Dorsal: spinothalamic tract
DR	DRC, DRD, DRI, DRL, DRV, PDR	8.37 to 8.56	PAG	Raphe pontis nucleus	Caudal: MnR Rostral: caudal linear nucleus of the raphe	4th ventricle caudally; cerebral aqueduct and PAG rostrally	N/A	Caudal: medial longitudinal fasciculus and LDTg Rostral: mRt and CTg

All anatomic nomenclature, abbreviations, and atlas plates are from Paxinos, G., Huang, X., Sengul, G., & Watson, C. (2012). Organization of Brainstem Nuclei. In J. K. Mai & G. Paxinos (Eds.), *The Human Nervous System* (3rd ed., pp. 260-327). Amsterdam: Elsevier Academic Press. N/A = not applicable. Anatomic abbreviations are provided in the Supplementary Material.

Table S3. Neuroanatomic Localization of Pontine Arousal Nuclei

Node	Component Nuclei	Atlas Plates	Rostral Boundary	Caudal Boundary	Ventral Boundary	Dorsal Boundary	Medial Boundary	Lateral Boundary
PnO	PnO	8.37 to 8.50	Ponto-mesencephalic junction	Mid-pons at the pontine reticular nucleus, caudal part	Caudal: B9 serotonin cells, trigeminothalamic tract and ML Rostral: decussation of SCP	Caudal: Dorsomedial tegmental area Rostral: MLF and LDTg	MnR	Caudal: CTg Rostral: CTg and SCP
PBC	MPB, MPBE, LPB, LPBC, LPBD, LPBE, LPBS	8.37 to 8.50	Ponto-mesencephalic junction	Mid-pons at the superior vestibular nucleus	CTg and ventrolateral tegmental area	SCP	* Caudal: LC and subcoeruleus nucleus Rostral: LC, LDTg, and CTg	** Lateral boundary of pons
MnR	MnR, PMnR	8.37 to 8.50	Ponto-mesencephalic junction	Mid-pons at the raphe pontis nucleus	Caudal: reticulotegmental nucleus Rostral: pontine nuclei, B9 serotonin cells, and decussation of the SCP	DR	N/A	PnO
LC	LC	8.37 to 8.50	Ponto-mesencephalic junction	Mid-pons at the superior vestibular nucleus	Caudal: subcoeruleus nucleus, dorsal part Rostral: LDTg	Caudal: central grey of the rhombencephalon Rostral: epicoeruleus nucleus	Caudal: central grey of the rhombencephalon Rostral: LDTg	PBC
LDTg	LDTg, LDTgV	8.41 to 8.50	Ponto-mesencephalic junction	Mid-pons at the central grey of the rhombencephalon	MLF, CTg, and PnO	Central grey of the rhombencephalon and LC	Central grey of the rhombencephalon, MLF, and DR	Caudal: LC and PBC Rostral: LC, PBC, and SCP

All anatomic nomenclature, abbreviations, and atlas plates are from Paxinos, G., Huang, X., Sengul, G., & Watson, C. (2012). Organization of Brainstem Nuclei. In J. K. Mai & G. Paxinos (Eds.), *The Human Nervous System* (3rd ed., pp. 260-327). Amsterdam: Elsevier Academic Press. N/A = not applicable. Anatomic abbreviations are provided in the Supplementary Material. * For the medial boundary of PBC, we refer to structures on the medial aspect of the medial component of PBC. The medial boundary of the lateral component of PBC is the SCP along its entire rostro-caudal extent. ** For the lateral boundary of PBC, we refer to structures on the lateral aspect of the lateral component of PBC. The lateral boundary of the medial component of PBC is the SCP along its entire rostro-caudal extent.

Table S4. Neuroanatomic Localization of Thalamic Arousal Nuclei

Node	Component Nuclei	Atlas Plates	Inferior Boundary	Superior Boundary	Anterior Boundary	Posterior Boundary	Medial Boundary	Lateral Boundary
IL	CL, CeM, PC, CD, CM, Pf, SPf, Fa	27 to 57	Centromedian nucleus of the thalamus	Anterior: anteroventral nucleus of the thalamus Posterior: dorsal superficial nucleus (laterodorsal nucleus) of the thalamus	Anterior border of thalamus Fasciculosus nucleus	Pulvinar	Medial dorsal thalamic nucleus	Pulvinar ventral lateral thalamic nucleus posteriorly and ventral anterior thalamic nucleus anteriorly
Ret	Rmc , Rpc	25 to 65	Zona incerta and subthalamic nucleus	Stria terminalis and white matter of the forebrain	Bed nucleus of stria terminalis	Crus of the fornix	Anterior: Ventral anterior nucleus of thalamus Posterior: Ventral lateral nucleus, lateral posterior nucleus, and pulvinar	White matter of the forebrain (internal capsule)
PaV	PaVr, PaVc	27 to 47	Anterior: rhomboid nucleus of thalamus Posterior: periventricular area of thalamus, intermediodorsal nucleus of thalamus, and intralaminar nuclei	Stria medullaris and velum interpositum	Supraoptic region of hypothalamus and fornix	Periventricular area of thalamus	Third ventricle	Anterior: fasciculosus nucleus of thalamus and anteromedial nucleus of thalamus Posterior: mediodorsal nucleus and intralaminar nuclei

All anatomic nomenclature, abbreviations, and atlas plates are from Ding, S.L. et al. (2016). Comprehensive cellular-resolution atlas of the adult human brain. *J Comp Neurol* **524** (16): 3127-3481. Anatomic abbreviations are provided in the Supplementary Material.

Table S5. Neuroanatomic Localization of Hypothalamic Arousal Nuclei

Node	Component Nuclei	Atlas Plates	Inferior Boundary	Superior Boundary	Anterior Boundary	Posterior Boundary	Medial Boundary	Lateral Boundary
TMN	TMN	34* to 40	Lateral tuberal nuclei and medial mammillary nucleus	Lateral hypothalamic area and substantia nigra, reticular part	Lateral hypothalamic area	Lateral hypothalamic area and retromammillary area	Anterior: lateral hypothalamic area and fornix Posterior: medial mammillary nucleus	Anterior: optic tract Posterior: substantia nigra, reticular part
LHA	LHAa**, LHAp, LHAtub	27 to 42	Anterior: optic tracts, supraoptic nucleus, retrochiasmatic nucleus, and interpeduncular cistern Posterior: TM and mammillary bodies	Anterior: dorsomedial hypothalamic nucleus, tuberal region of hypothalamus, and fornix Posterior: ventral anterior nucleus of thalamus, mammillo-tegmental tract and zona incerta	Preoptic region of hypothalamus	Midbrain	Anterior: tuberal region of hypothalamus Posterior: mammillary region of hypothalamus, mammillothalamic tract	Anterior: BNM/SI, forebrain white matter Posterior: Subthalamic nucleus and substantia nigra reticular part
SUM	SUM	35 to 40	Mammillary body and mammillothalamic tract	Posterior hypothalamic nucleus	Posterior hypothalamic nucleus and mammillary peduncle	Posterior hypothalamic nucleus	Posterior hypothalamic nucleus	Anterior: LHA Posterior: TMN and mammillary body

All anatomic nomenclature, abbreviations, and atlas plates are from Ding, S.L. et al. (2016). Comprehensive cellular-resolution atlas of the adult human brain. *J Comp Neurol* **524** (16): 3127-3481. N/A = not applicable. Anatomic abbreviations are provided in the Supplementary Material.
* From plates 29 to 33, TM is fully enveloped within LHA and cannot be reliably distinguished from LHA. Therefore, we operationally define the anterior boundary of the TM node at plate 34. ** LHAa is not depicted in the Ding atlas.

Table S6. Neuroanatomic Localization of Basal Forebrain Arousal Nuclei

Node	Component Nuclei	Atlas Plates	Inferior Boundary	Superior Boundary	Anterior Boundary	Posterior Boundary	Medial Boundary	Lateral Boundary
DBB	NDBv, NDBh, dib	19 to 23	Anterior: subgenual division of anterior cingulate cortex Posterior: basal cisterns	Anterior: medial septal nucleus Posterior: preoptic region of hypothalamus	subgenual division of anterior cingulate cortex	Preoptic region of hypothalamus	Anterior: basal cisterns Posterior: preoptic region of hypothalamus	Anterior: septal nuclei Posterior: NBM/SI
BNM/SI	BNMl, BNMm, SI-pc, SI-nc	19 to 45	Anterior: forebrain white matter, subgenual division of anterior cingulate cortex Middle: basal cisterns Posterior: amygdaloid complex	Anterior: ventral pallidus, olfactory tubercle Middle: sublenticular extended amygdala, anterior commissure Posterior: globus pallidus	Olfactory tubercle, forebrain white matter	Optic tract, amygdaloid complex, forebrain white matter,	Anterior: diagonal band Middle: LHA Posterior: optic tract	Anterior: lateral olfactory area Middle: putamen, anterior commissure Posterior: amygdalostriatal transition area

All anatomic nomenclature, abbreviations, and atlas plates are from Ding, S.L. et al. (2016). Comprehensive cellular-resolution atlas of the adult human brain. *J Comp Neurol* **524** (16): 3127-3481. Anatomic abbreviations are provided in the Supplementary Material.

Table S7. Interspecimen Variance in Brainstem-Thalamic Projection Connectivity Probabilities

Nodes	IL			PaV			Ret		
	S2	S3	Mean	S2	S3	Mean	S2	S3	Mean
mRt	0.60	3.05	1.82	0.4	3.07	1.72	1.94	3.96	2.95
VTA	0.03	0.70	0.36	0	0.75	0.39	0.09	0.80	0.44
PAG	0.25	3.26	1.75	1.7	6.33	4.02	2.14	0.67	1.40
PTg	0.02	0.72	0.37	0	0.80	0.40	0.04	0.47	0.26
DR	0.001	0.16	0.08	0	0.08	0.04	0.002	0.20	0.10
PnO	0	0.10	0.05	0	0.003	0.001	0	0.34	0.17
PBC	0	0.25	0.13	0	0.01	0.003	0	0.49	0.25
MnR	0	0.11	0.05	0	0.003	0.001	0	0.3	0.15
LC	0	0.10	0.05	0	0.003	0.002	0	0.1	0.05
LDTg	0	0.07	0.04	0	0.002	0.001	0	0.10	0.05

All connectivity probability measurements are multiplied by 100 and reported as percentages. Anatomic abbreviations are provided in the Supplementary Material. Highlighted in RED are connections that failed that confidence interval test. S2 = Specimen 2; S3 = Specimen 3.

Table S8. Interspecimen Variance in Brainstem-Hypothalamic Projection Connectivity Probabilities

Nodes	TM			LHA			SUM		
	S2	S3	Mean	S2	S3	Mean	S2	S3	Mean
mRt	1.15	1.47	1.31	3.79	3.48	3.64	0.76	0.93	0.85
VTA	10.20	18.71	14.45	22.57	24.29	23.43	7.85	23.48	15.66
PAG	0.55	2.82	1.69	3.02	2.74	2.88	0.43	2.39	1.41
PTg	9.96	9.57	9.77	9.98	13.48	11.73	5.89	8.88	7.36
DR	1.49	3.76	2.62	2.80	2.79	2.79	1.43	4.47	2.95
PnO	1.84	1.70	1.77	2.57	1.61	2.09	1.37	2.85	2.11
PBC	3.99	4.05	4.02	4.20	4.73	4.46	3.17	3.77	3.47
MnR	0.94	1.01	0.98	1.07	0.71	0.89	1.10	2.01	1.55
LC	0.88	1.91	1.39	1.45	2.81	2.13	1.05	2.44	1.74
LDTg	0.36	1.36	0.86	0.75	1.96	1.36	0.56	2.26	1.41

All connectivity probability measurements are multiplied by 100 and reported as percentages. Anatomic abbreviations are provided in the Supplementary Material. Highlighted in RED are connections that failed that confidence interval test. S2 = Specimen 2; S3 = Specimen 3.

Table S9. Interspecimen Variance in Brainstem-Basal Forebrain Projection Connectivity Probabilities

Nodes	DBB			BNM/SI		
	S2	S3	Mean	S2	S3	Mean
mRt	0.03	0.07	0.05	1.23	1.52	1.37
VTA	0.08	0.006	0.04	6.61	10.93	8.77
PAG	0.07	0.06	0.07	1.01	0.92	0.96
PTg	0.01	0.01	0.01	1.91	6.78	4.35
DR	0.04	0.04	0.04	0.80	1.12	0.96
PnO	0.003	0.001	0.002	0.71	0.72	0.71
PBC	0.009	0.006	0.007	0.95	2.22	1.58
MnR	0.002	0.001	0.001	0.29	0.35	0.32
LC	0.01	0.02	0.01	0.42	1.32	0.87
LDTg	0.005	0.006	0.006	0.22	0.97	0.59

All connectivity probability measurements are multiplied by 100 and reported as percentages. Anatomic abbreviations are provided in the Supplementary Material. Highlighted in RED are connections that failed that confidence interval test. S2 = Specimen 2; S3 = Specimen 3.

Table S10. Interspecimen Variance in Brainstem-DMN Projection Connectivity Probabilities

Nodes	PMC			MPFC			IPL			LT			MT		
	S2	S3	Mean	S2	S3	Mean	S2	S3	Mean	S2	S3	Mean	S2	S3	Mean
mRt	0.59	0.14	0.37	0.1	0.007	0.04	0.01	0.03	0.02	0	0.01	0.004	0.24	1.34	0.79
VTA	0.24	0.22	0.23	0.1	0.004	0.04	0.002	0.02	0.01	0	0.01	0.002	0.01	0.47	0.24
PAG	0.93	0.29	0.61	0.1	0.006	0.05	0.01	0.03	0.02	0	0.004	0.002	0.21	0.03	0.12
PTg	0.22	0.07	0.15	0	0.002	0.006	0	0.007	0.004	0	0.01	0.003	0	0.83	0.42
DR	0.16	0.18	0.17	0.1	0.003	0.04	0	0.02	0.008	0	0.01	0.005	0	2.03	1.02
PnO	0.001	0.06	0.03	0	0.005	0.003	0	0.03	0.01	0	0.01	0.006	0	6.21	3.11
PBC	0	0.01	0.006	0	0.001	0.001	0	0.03	0.01	0	0.02	0.01	0	8.66	4.33
MnR	0	0.01	0.007	0	0.004	0.002	0	0.01	0.01	0	0.01	0.005	0	6.15	3.08
LC	0	0.002	0.001	0	0	0.0	0	0.003	0.002	0	0.005	0.002	0	1.36	0.68
LDTg	0	0.001	0.001	0	0	0.0	0	0.003	0.002	0	0.004	0.002	0	1.30	0.65

All connectivity probability measurements are multiplied by 100 and reported as percentages. Anatomic abbreviations are provided in the Supplementary Material. Highlighted in RED are connections that failed that confidence interval test. S2 = Specimen 2; S3 = Specimen 3.

Table S11. Interspecimen Variance in Left-Sided Association Connectivity Probabilities

Nodes	mRt_L			PTg_L			PnO_L			PBC_L			LC_L			LDTg_L		
	S2	S3	Mean	S2	S3	Mean	S2	S3	Mean	S2	S3	Mean	S2	S3	Mean	S2	S3	Mean
mRt_L				23.00	19.36	21.01	0.42	0.01	0.21	0.35	0.03	0.19	0.10	0.72	0.41	0.06	0.11	0.08
PTg_L	22.67	19.36	21.01				1.57	0.05	0.81	1.53	3.47	2.50	0.93	0.04	0.49	0.46	0.02	0.24
PnO_L	0.42	0.01	0.21	1.60	0.05	0.81				27.60	40.93	34.26	18.47	3.34	10.90	14.40	1.93	8.16
PBC_L	0.35	0.03	0.19	1.50	3.47	2.50	27.60	40.93	34.26				17.57	30.81	24.19	6.21	28.30	17.26
LC_L	0.10	0.72	0.41	0.90	0.04	0.49	18.47	3.34	10.90	17.57	30.81	24.19				52.00	58.09	55.05
LDTg_L	0.06	0.11	0.08	0.50	0.02	0.24	14.40	1.93	8.16	6.21	28.30	17.26	52.00	58.09	55.05			

All connectivity probability measurements are multiplied by 100 and reported as percentages. Anatomic abbreviations are provided in the Supplementary Material. Highlighted in RED are connections that failed that confidence interval test. S2 = Specimen 2; S3 = Specimen 3.

Table S12. Interspecimen Variance in Right-Sided Association Connectivity Probabilities

Nodes	mRt_R			PTg_R			PnO_R			PBC_R			LC_R			LDTg_R		
	S2	S3	Mean	S2	S3	Mean	S2	S3	Mean	S2	S3	Mean	S2	S3	Mean	S2	S3	Mean
mRt_R				7.52	21.34	14.43	3.35	0.17	1.76	24.88	17.93	21.41	28.29	27.89	28.09	11.23	5.28	8.25
PTg_R	7.52	21.34	14.43				2.81	0.75	1.78	45.81	58.66	52.23	2.12	3.41	2.76	0.65	0.17	0.41
PnO_R	3.35	0.17	1.76	2.81	0.75	1.78				2.94	2.44	2.69	1.43	3.43	2.43	2.21	1.65	1.93
PBC_R	24.88	17.93	21.41	45.81	58.66	52.23	2.94	2.44	2.69				17.86	6.80	12.33	0.68	0.26	0.47
LC_R	28.29	27.89	28.09	2.12	3.41	2.76	1.431	3.43	2.43	17.86	6.80	12.33				50.79	31.60	41.19
LDTg_R	11.23	5.28	8.25	0.65	0.17	0.41	2.21	1.65	1.93	0.68	0.26	0.47	50.79	31.60	41.19			

All connectivity probability measurements are multiplied by 100 and reported as percentages. Anatomic abbreviations are provided in the Supplementary Material. Highlighted in RED are connections that failed that confidence interval test. S2 = Specimen 2; S3 = Specimen 3.

Table S13. Interspecimen Variance in Midline Association Connectivity Probabilities

Nodes	VTA			PAG			DR			MnR		
	S2	S3	Mean	S2	S3	Mean	S2	S3	Mean	S2	S3	Mean
mRt_L	16.29	13.77	15.03	50.00	9.37	29.83	10.20	3.99	7.09	0.66	0.01	0.33
PTg_L	3.72	1.95	2.84	4.60	0.62	2.63	2.19	0.07	1.13	2.55	0.02	1.29
PnO_L	4.49	0.02	2.25	0.10	0.01	0.07	8.66	6.51	7.58	62.61	68.11	65.36
PBC_L	0.10	0.03	0.07	0	0.01	0.01	3.38	20.34	11.86	22.09	36.38	29.23
LC_L	0.25	0.02	0.13	0	0.03	0.02	8.85	18.12	13.49	25.24	5.98	15.61
LDTg_L	0.26	0.01	0.13	0	0.01	0.01	6.56	12.25	9.41	21.65	4.60	13.13
mRt_R	9.42	13.86	11.64	50.00	20.35	35.29	10.00	5.79	7.90	0.14	0.01	0.07
PTg_R	7.89	8.06	7.98	1.10	8.75	4.91	1.25	2.80	2.02	0.25	0.02	0.14
PnO_R	6.06	0.01	3.04	0.50	0.01	0.27	19.05	7.48	13.26	64.63	64.02	64.32
PBC_R	2.58	0.21	1.40	0.50	0.45	0.47	8.42	15.38	11.90	7.33	49.39	28.36
LC_R	1.30	0.12	0.71	0.30	0.02	0.14	14.03	18.80	16.42	8.81	0.91	4.86
LDTg_R	0.58	0.01	0.30	0.10	0.01	0.04	8.42	15.82	12.12	4.64	1.31	2.98
VTA				14.06	34.95	24.51	27.28	17.34	22.31	6.69	0.01	3.35
PAG	14.06	34.95	24.51				26.83	26.44	26.63	0.27	0.01	0.14
DR	27.28	17.34	22.31	26.83	26.44	26.63				19.63	13.34	16.49
MnR	6.69	0.01	3.35	0.27	0.01	0.14	19.63	13.34	16.49			

All connectivity probability measurements are multiplied by 100 and reported as percentages. Anatomic abbreviations are provided in the Supplementary Material. Highlighted in RED are connections that failed that confidence interval test. S2 = Specimen 2; S3 = Specimen 3.

Table S14. Interspecimen Variance in Commissural Connectivity Probabilities

Nodes	mRt_R			PTg_R			PnO_R			PBC_R			LC_R			LDTg_R		
	S2	S3	Mean	S2	S3	Mean	S2	S3	Mean	S2	S3	Mean	S2	S3	Mean	S2	S3	Mean
mRt_L	35.25	0.21	17.73	0.70	0.11	0.41	0.78	0.01	0.40	0.17	0.01	0.09	0.32	0.004	0.16	0.05	0.003	0.02
PTg_L	4.28	0.13	2.20	3.90	0.14	2.03	2.29	0.02	1.16	0.62	0.03	0.33	1.46	0.01	0.74	0.20	0.02	0.11
PnO_L	0.04	0.02	0.03	0.10	0.04	0.06	33.46	59.52	46.49	3.23	49.19	26.21	4.45	1.02	2.73	2.33	1.25	1.79
PBC_L	0.01	0.01	0.01	0	0.06	0.03	9.45	31.87	20.66	0.10	48.70	24.40	0.55	25.48	13.01	0.13	27.30	13.72
LC_L	0.01	0.01	0.01	0	0.03	0.02	20.60	2.56	11.58	0.38	23.72	12.05	3.35	30.35	16.85	1.02	38.11	19.56
LDTg_L	0.01	0.002	0.004	0	0.01	0.01	18.68	2.03	10.35	0.49	17.32	8.91	3.47	25.04	14.26	2.25	43.88	23.07

All connectivity probability measurements are multiplied by 100 and reported as percentages. Anatomic abbreviations are provided in the Supplementary Material. Highlighted in RED are connections that failed that confidence interval test. S2 = Specimen 2; S3 = Specimen 3.